Optics & Laser Technology 43 (2011) 1499–1503

Contents lists available at ScienceDirect

Optics & Laser Technology

journal homepage: www.elsevier.com/locate/optlastec

Experimental investigation of the effect of ambient pressure on laser-induced bubble dynamics

Bei-bei Li, Hong-chao Zhang, Jian Lu*, Xiao-wu Ni

School of Science, Nanjing University of Science and Technology, Nanjing 210094, China

ARTICLE INFO

Article history:
Received 16 November 2010
Received in revised form
3 April 2011
Accepted 4 May 2011

Keywords:
Ambient pressure
Optical beam deflection
Cavitation bubble

ABSTRACT

The effect of ambient pressure on the dynamics of laser-induced bubbles was investigated by a fiber-optic diagnostic technique based on probe beam deflection (PBD). The experimental criterion for judging the maximum bubble radius is modified to the average value of the detecting distances at which the characteristic waveform signals appear. The ambient pressure affects the maximum radius and collapse of bubble strongly. The experimental results indicate that the maximum bubble radius and the collapse time both decrease nonlinearly while the ambient pressure increases linearly, and the decreasing velocities of them are smaller at a larger ambient pressure. The predicted value of collapse time has a good agreement with experiment at larger ambient pressure.

1. Introduction

Cavitation bubbles occur when the local pressure is lower than the saturated vapor pressure at ambient temperature [1]. The interest in cavitation bubbles in liquids arises mainly from their special consequences such as the liquid-jet, cavitation noise and high pressure and temperature induced by bubble collapse. In medical applications the cavitation bubbles, as a collateral effect of optical breakdown, also bring certain unwanted effects. However, the effects of bubbles also lead to some useful outcomes, for e.g. the collapse of a bubble is helpful in the treatment of waste water and cleaning of metal surfaces [1–5]. Therefore, many theoretical and experimental reports have been published in this area.

On the one hand, cavitation bubbles could be induced in different ways in experiments using adopt spark discharge [3], ultrasonics [6,7] and laser pulses [5,8–11]. In model experiments the cavitation bubbles are generally induced by laser pulses, because the creation time and inception point of the laser-induced bubble is easy to control. On the other hand, the commonly used optical methods for measuring cavitation bubbles include high-speed photography [2], schlieren photography [12], shadow photography [5] and the measurements based on probe beam deflection (PBD) [5,10] or Mie scattering [13]. Methods based on hydrophones have also been adopted to measure the shockwave [14]. The technique based on the PBD allows for simultaneous measurements of the cavitation bubble and the shock waves, and the measurement noise can also be reduced by a method proposed in Ref. [5]. Furthermore, the bubble oscillations are measured with one-dimensional PBD scanning, which has many advantages such as low cost, simple structure and high-frequency response (more than 10 MHz).

Rayleigh [15] first roughly described the dynamics of the spherical bubble in an infinite, incompressible and nonviscous liquid in 1917. Then in 1949, Plesset completed Rayleigh's model and derived the Rayleigh–Plesset equation [5,16]. Following this work, many researchers have modified the bubble model and discussed the effects of other factors (viscidity, surface tension and compressibility of liquid, heat conduction, mass transfer effects, etc.) [1]. Moreover, the liquid surrounding the bubble may have different ambient pressures, which is also an influential factor of bubble's dynamics. Kondic et al. [6] and Dan et al. [7] have discussed the effects of ambient pressure on bubble dynamics in their study of single-bubble sonoluminescence (SBSL). Lu Xin-Pei et al. [3] investigated the bubble oscillation and the peak pressure of the shockwave when the ambient pressure increased from 1 to 100 atm.

However, the above reports do not include detailed investigation of the maximum radius and collapse time of bubbles in different ambient pressures. In this study, detailed investigations were undertaken on the effects of ambient pressure on the maximum bubble radius and collapse time. It is difficult to satisfy the experimental criteria proposed in Ref. [10] for judging the maximum bubble radius in the measurement by means of PBD. So these experimental criteria were modified in our experiments. The maximum bubble radius, collapse time and shockwave of each oscillation period were obtained from the waveforms induced by bubble's motion using these experimental criteria and the criteria of collapse time.

* Corresponding author.
E-mail address: libeibei1015@hotmail.com (J. Lu).

0030-3992/$ - see front matter © 2011 Elsevier Ltd. All rights reserved.
doi:10.1016/j.optlastec.2011.05.016

2. Theoretical Basis

2.1. Collapse time of bubble

The motion of a spherical bubble in an infinitely large, incompressible and nonviscous liquid is roughly described by the Rayleigh–Plesset equation [1,5,16], which was derived from the equation of continuity and the Navier–Stokes equation.

$$R\ddot{R}+\frac{3}{2}\dot{R}^2=\frac{p(R)-p_0(t)}{\rho} \tag{2.1}$$

Here, R is the radius of bubble, $p(R)$ is the pressure at the bubble boundary, $p_0(t)$ is the pressure of surrounding liquid (ambient pressure), ρ is the density of liquid and its value is 1000 kg/m^3 for the distilled water used in our experiment. In the special case, the Eq. (2.1) can be rearranged into Eq. (2.2) with the assumption that $p_0(t)=p_0$ (constant), $p(R)=p_v$ (p_v is saturated vapor pressure of liquid at 20 °C) and $p_v \ll p_0$.

$$\frac{1}{2R^2\dot{R}}\frac{d}{dt}(R^3\dot{R}^2)=-\frac{p_0}{\rho} \tag{2.2}$$

We were able to integrate Eq. (2.2) to obtain the velocity of bubble wall as shown in Eq. (2.3).

$$\dot{R}=\frac{dR}{dt}=\sqrt{\frac{2}{3}\frac{p_0}{\rho}\left(\frac{R_{\max}^3}{R^3}-1\right)} \tag{2.3}$$

Here, $R_{\max}$ is the maximal radius of bubble. The bubble's collapse time, T_C, required for total collapse from $R=R_{\max}$ to $R=0$, can be obtained by integrating Eq. (2.3), and is expressed as [1,9,11,15]

$$T_C=\sqrt{\frac{3}{2}\frac{\rho}{p_0}}\int_0^{R_{\max}}\left(\frac{R_{\max}^3}{R^3}-1\right)^{-(1/2)}dR\approx 0.915\ R_{\max}\sqrt{\frac{\rho}{p_0}} \tag{2.4}$$

This equation has a good agreement with the condition of a bubble in an infinite liquid. However, when cavitation bubble collapse occurs near the boundaries such as rigid and free boundaries, it does not maintain a spherical shape and the collapse time will be prolonged or shortened [11]. Consequently Eq. (2.4) is no longer appropriate. According to the modified Rayleigh's model by Rattray [17], the prolongation factor κ, defined as the ratio between the collapse time of a bubble collapsing near a rigid boundary T_C' and the Rayleigh's collapse time of a equivalent spherical bubble in an infinite liquid T_C, can be roughly described by the equation.

$$\kappa=\frac{T_C'}{T_C}=1+0.41\frac{1}{2\gamma} \tag{2.5}$$

Here, $\gamma=l/R_{\max}$ is the dimensionless distance parameter, where l is the distance of the center of the bubble from the boundary. However, Eq. (2.5) is not suitable for very small γ, because it predicts that the value of prolongation factor κ approaches infinity while the dimensionless distance parameter γ approaches zero. The investigation of Godwin [18] also pointed out that the prolongation factors are in fair agreement with the theoretical predictions while γ is equal to or larger than 1, but they (or collapse times) are much smaller than predicted while γ is less than 1 and the values of them decreases with decreasing of γ. As the previous work [8] of our group, γ is in range of 0.1 in this paper. According to Godwin's work, the prolongation factor κ is approximately equal to 1.14 when γ is equal to 0.1 [18]. Simultaneous Eqs. (2.4) and (2.5), the Eq. (2.6) of the relationship between collapse time and ambient pressure at $\gamma=0.1$ can be obtained.

$$T_C'=1.0431R_{\max}\sqrt{\frac{\rho}{p_0}} \tag{2.6}$$

This equation show that the collapse time of bubble is proportional to the maximum radius of bubble $R_{\max}$ and its square is inversely proportional to ambient pressure p_0.

2.2. Energy of bubble

The energy of cavitation bubble E_b is proportional to the cube of its maximum radius $R_{\max}$ [5,19,20].

$$E_b=\frac{4}{3}\pi R_{\max}^3 p_0 \tag{2.7}$$

Here, p_0 is the ambient pressure of bubble and its value is in range of 1–3.5 atm in this paper. In addition, some researchers indicated that the cavitation bubble's energy is also approximately proportional to the energy of the laser pulse E_l [5].

$$E_b=\eta E_l \tag{2.8}$$

Here, η is the scale of laser pulse energy converted into cavitation bubble's energy. Its value is affected by laser pulse energy [5] or other factors. In this experiment, the energy of laser pulse is constant and we assumed that η is only affected by laser pulse energy. So we could just pay attention to the relationship between ambient pressure and $R_{\max}$ at constant laser energy in our study. Simultaneously from Eqs. (2.7) and (2.8), the Eq. (2.9) of bubble's maximum radius is obtained.

$$R_{\max}^3=\frac{3\eta E_l/4\pi}{p_0} \tag{2.9}$$

This equation shows that the cube of bubble' maximum radius is inversely proportional to ambient pressure p_0, while the relationship between η and ambient pressure p_0 is ignored.

3. Experimental setup

The experimental arrangement is outlined in Fig. 1. The system to induce a bubble in liquid was made up of 1–8 in Fig. 1.

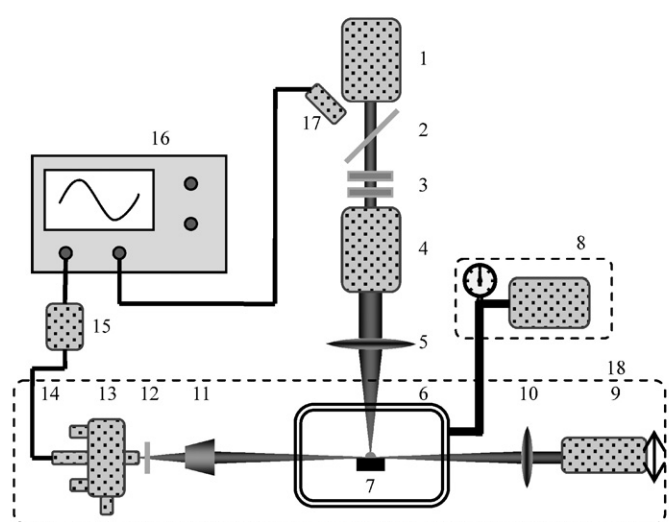

Fig. 1. Sketch of experimental setup: (1) Q-switched Nd:YAG laser ($\lambda=1.06$ μm, pulse duration 10 ns); (2) beam splitter; (3) attenuator group; (4) expanded and collimated beam lens combination; (5) convex lens ($f_1=80$ mm); (6) pressure vessel (120 mm × 120 mm × 120 mm); (7) aluminum target; (8) pressure-handling system fitted a pressure gage (Leierda YB-150B, range 0–0.6 MPa, accuracy grade 0.25); (9) He–Ne laser (power 5 mW, $\lambda=0.63$ μm); (10) convex lens ($f_2=80$ mm); (11) microscope objective (20 ×); (12) interference filter ($\lambda=0.63$ μm); (13) five-dimensional fiber-regulating stand (0.1 μm spatial resolution); (14) single-mode optical fiber; (15) photomultiplier (Hamamatsu H5773 with 2 ns rise time); (16) digital oscilloscope (Tektronix THS730A); (17) PIN photodiode (with 0.1 ns rise time); (18) two-dimensional platform (10 μm spatial resolution).